Applied Research in Science and Technology 6(1): 173-190 2026

Contents lists available at openscie.com
E-ISSN: 2776-7205
Applied Research in Science and Technology
DOI: 10.33292/areste.v6i1.165
Journal homepage: https://areste.org/index.php/oai

Effects of Sugarcane Molasses Concentration and Cultivation Strategy on Bacterial Cellulose Yield and Properties

Nurijawati Nurijawati[1,2*], Sarkono Sarkono[1,3], Dhony Hermanto[4]

[1] Master's Program in Biology, Faculty of Mathematics and Natural Sciences, University of Mataram, Mataram, Indonesia
[2] Laboratory of Biology, Faculty of Mathematics and Natural Sciences, University of Mataram, Mataram, Indonesia
[3] Department of Biology, Faculty of Mathematics and Natural Sciences, University of Mataram, Mataram, Indonesia
[4] Department of Chemistry, Faculty of Mathematics and Natural Sciences, University of Mataram, Mataram, Indonesia

*Correspondence E-mail: nurrijawati19@staff.unram.ac.id

ARTICLE INFO

Article History:
Received 2 August 2026
Revised 21 October 2026
Accepted 22 October 2026
Published 28 October 2026

Keywords:
Bacterial cellulose,
Fermentation,
Gluconacetobacter sp. SAL-53,
Physicochemical properties,
Sugarcane molasses.

ABSTRACT

Background: Bacterial cellulose (BC) is a promising biomaterial whose yield and physicochemical properties depend on cultivation conditions.
Aims: This study investigated the combined effects of sugarcane molasses concentration and cultivation strategy on BC yield and material properties using *Gluconacetobacter* sp. SAL-53
Methods: A 4 × 4 factorial design was employed, comprising four molasses concentrations (3, 6, 9, and 12%, w/v) and four cultivation conditions: static culture and agitation at 100, 150, and 200 rpm. BC was produced for 14 days and evaluated for dry yield, tensile strength, *Young's modulus*, water absorption capacity, water-holding capacity, electrical conductivity, biodegradability, surface morphology, and chemical structure.
Results: The highest dry BC yield was 51.50 ± 0.26 g L^{-1} at 6% molasses and 100 rpm. Agitation at 200 rpm produced BC with a tensile strength of 52.80 MPa and a Young's modulus of 720.40 MPa, with comparatively high electrical conductivity. FTIR analysis showed characteristic cellulose-associated functional groups across the analyzed samples, while SEM revealed differences in surface morphology. Two-way ANOVA and Tukey's Test indicated a significant overall effect of the experimental treatments on the combined physicochemical response ($p < 0.001$).
Conclusion: Molasses concentration and cultivation strategy significantly influenced BC yield and physicochemical properties. The molasses concentration of 6% at 100 rpm agitation is the optimum condition for yield, whereas 200 rpm produced BC with greater mechanical strength and electrical conductivity. These findings show that molasses is a feasible low-cost substrate and that cultivation strategy can be adjusted to obtain BC suited to different applications.

To cite this article: Nurijawati, N., Sarkono, S., Hermanto, D. (2026). Effects of Sugarcane Molasses Concentration and Cultivation Strategy on Bacterial Cellulose Yield and Properties. *Applied Research in Science and Technology*, 6(1), 173-190.

This article is under a Creative Commons Attribution-ShareAlike 4.0 International (**CC BY-SA 4.0**) License. Creative Commons Attribution-ShareAlike 4.0 International License Copyright ©2026 by author/s

1. Introduction

Bacterial cellulose (BC) is a microbial biopolymer that has attracted considerable interest because of its high purity, mechanical strength, water-holding capacity, and distinctive nanofibrillar structure (Kumar *et al.*, 2025; Wang *et al.*, 2026). Unlike plant-derived cellulose, BC is produced without the

lignin and hemicellulose commonly associated with plant cell walls. These characteristics make BC attractive for a range of material and biotechnological applications (Amorim *et al.,* 2024; Çalhan & Hasanoğlu, 2026). However, the cost of conventional fermentation media, particularly purified carbon sources such as glucose, remains a challenge for economical BC production (Alidu & Alexander, 2026; Hapsari *et al.,* 2024; Rezaei *et al.,* 2025). On the other hand, the utilization of renewable agro-industrial by-products is an important approach to developing more resource-efficient BC production systems.

Sugarcane molasses is a potential alternative carbon source because it contains fermentable sugars and is available as a by-product of the sugar industry (Parchaykina *et al.,* 2025; Tyagi & Suresh, 2016). However, its suitability for BC production depends not only on its availability but also on its concentration and the composition of the fermentation medium (Mirshafiei *et al.,* 2026). Excessive or insufficient substrate concentrations may alter microbial growth and cellulose biosynthesis, while the non-sugar constituents of molasses may also influence fermentation performance (Ji *et al.,* 2016; López-lópez *et al.,* 2026; Oesef *et al.,* 2024). Therefore, identifying an appropriate molasses concentration is important for achieving a favourable BC yield, particularly because increasing substrate concentration does not necessarily result in higher BC formation.

In addition to medium composition, cultivation strategy can influence BC yield and material characteristics. Static and agitated cultivation can generate different mixing and mass-transfer conditions, which may influence BC formation, morphology, and functional properties. Such differences may influence BC yield, morphology, mechanical performance, and hydration behaviour (Andrade *et al.,* 2020; Lahiri *et al.,* 2021; Turganova *et al.,* 2025). Nevertheless, BC yield alone does not fully describe material quality, because the resulting physicochemical properties are also relevant to its potential applications. Although previous studies have examined carbon sources and cultivation conditions separately, their combined effects on BC yield and material properties remain insufficiently characterised, particularly for locally isolated strains such as *Gluconacetobacter* sp. SAL-53 (Gomes *et al.,* 2013; Sarkono *et al.,* 2014).

Rather than examining molasses concentration or cultivation strategy in isolation, this study systematically evaluated their combined effects on BC yield and material properties using the locally isolated strain *Gluconacetobacter* sp. SAL-53. The study employed a 4 × 4 factorial design comprising four molasses concentrations (3, 6, 9, and 12%, w/v) and four cultivation conditions: static culture and agitation at 100, 150, and 200 rpm. BC was evaluated based on dry yield, mechanical properties, water absorption capacity, water-holding capacity, electrical conductivity, biodegradability, surface morphology, and chemical structure. Rather than examining molasses concentration or cultivation strategy in isolation, this study systematically evaluated their combined effects on BC yield and material properties using the locally isolated strain *Gluconacetobacter* sp. SAL-53.

2. Methods

2.1 Materials

Gluconacetobacter sp. SAL-53, a BC-producing strain, was obtained from the culture collection of the Biology Laboratory, University of Mataram, Indonesia. Sugarcane molasses was used as the principal carbon source and was obtained from a sugar-processing industry in Klaten, Indonesia. The molasses contained 17.39% total sugar and 14.95% reducing sugar. Ammonium sulphate ($(NH_4)_2SO_4$; Sigma-Aldrich, USA) was used as the nitrogen source, while sodium hydroxide (NaOH; Merck, Germany) was used for alkaline purification of the harvested BC. All chemicals and reagents were of analytical grade and prepared using distilled water. Glucose (2.0%, w/v; Merck, Germany), yeast extract (0.5%, w/v; HiMedia Laboratories, India), bacteriological peptone (0.5%, w/v; HiMedia Laboratories, India), disodium hydrogen phosphate (Na_2HPO_4; 0.15%, w/v; Merck, Germany), and citric acid (0.5%, w/v; Merck, Germany) were used to prepare. Hestrin–Schramm (HS) medium was used for bacterial activation and inoculum preparation. The medium contained glucose, yeast extract, peptone, citric acid,

and disodium hydrogen phosphate. The initial pH of the medium was adjusted to 5.0 before sterilisation. Unless otherwise stated, culture media and solutions were sterilised by autoclaving at 121 °C for 15 min.

2.2 Bacterial Strain and Inoculum Preparation

Gluconacetobacter sp. SAL-53 was activated in HS medium prior to fermentation. A fresh bacterial culture was inoculated into 500 mL of sterile HS broth and incubated at 30°C for 96 hours under the specified conditions for inoculum development. The actively growing culture obtained was subsequently utilised as the inoculum for bacterial cellulose (BC) production. The inoculum was introduced into the production medium at a volume of 10% (v/v). All inoculation procedures were conducted aseptically to minimise the risk of contamination during the fermentation process.

2.3 Experimental Design and BC Production

A 4 × 4 factorial experimental design was employed to evaluate the effects of molasses concentration and cultivation strategy on BC yield and functional properties. The first factor was sugarcane molasses concentration at four levels: 3, 6, 9, and 12% (w/v). The second factor was cultivation strategy at four levels: static cultivation and orbital shaking at 100, 150, and 200 rpm. Thus, 16 treatment combinations were evaluated. The fermentation working volume was 100 mL for each treatment combination, using a 250 mL flask with a cotton plug.

For each treatment, sugarcane molasses was diluted with distilled water to the designated concentration, followed by the addition of ammonium sulphate. The initial pH of the production medium was adjusted to 5.0 before sterilisation. The medium was autoclaved at 121°C for 15 min and cooled to approximately 30°C before inoculation with 10% (v/v) of the prepared *Gluconacetobacter* sp. SAL-53 inoculum. Cultures were incubated at 30°C for 14 days. Static cultures were maintained without mechanical agitation, whereas agitated cultures were incubated on an orbital shaker at 100, 150, or 200 rpm (Lahiri *et al.,* 2021; Sarkono *et al.,* 2014). Three independent fermentation cultures were prepared for each treatment combination and were considered biological replicates.

2.4 Determination of BC yield

After 14 days of cultivation, BC pellicles were harvested from the culture medium and washed repeatedly with distilled water. The harvested pellicles were subsequently purified using 2% (w/v) NaOH to remove bacterial cells and non-cellulosic residues. Following alkaline treatment, the BC pellicles were thoroughly washed with distilled water until the washing solution approached neutral pH. The purified BC pellicles were dried at 30°C until a constant mass was obtained and subsequently weighed using an analytical balance. Because the measured response represented the dry BC recovered at the end of the 14-day cultivation period, the response variable was expressed as BC yield rather than fermentation productivity. BC yield was calculated according to Eq. (1).

$$Y_{BC}\ (g\ L^{-1}) = \frac{m_{BC}\ (g)}{V_{f(L).}} \qquad (1)$$

where Y_{BC} is the BC yield (g L^{-1}), m_{BC} is the dry mass of purified BC (g), and V_f is the fermentation working volume (L).

2.5 Mechanical Properties of BC

The mechanical properties of the BC membranes were evaluated in terms of tensile strength and Young's modulus using a universal testing machine (RTG-1310, AND, Japan). Purified BC samples were dried under controlled conditions and cut into rectangular specimens prior to testing. Specimen dimensions and thickness were measured before analysis. Tensile testing was conducted at a constant crosshead speed of 1 mm min^{-1}. Tensile strength was calculated from the maximum stress recorded

before specimen failure, whereas *Young's modulus* was obtained from the slope of the linear region of the stress–strain curve.

2.6 Water Absorption Capacity (WAC) and Water-Holding Capacity (WHC)

WAC was determined using dried BC specimens with a known initial mass. Each specimen was immersed in distilled water for specific intervals. After immersion, excess surface water was gently removed before weighing. WAC was calculated using Eq. (2).

$$\mathrm{WAC}\ (\%) = \frac{m_t - m_0}{m_0} \times 100\% \qquad (2)$$

where m_0 denotes the initial dry mass of the BC specimen, while m_t signifies the mass of the specimen following the specified period of water immersion. Measurements were conducted utilising biological replicates from each treatment.

WHC was determined from purified BC samples with a known wet mass. The samples underwent centrifugation according to the experimental conditions outlined in the original procedure, and the mass retained after centrifugation was recorded. WHC was calculated based on the amount of water retained by the BC in relation to its initial water content. Three independent biological replicates were assessed for each treatment.

2.7 Electrical Conductivity

Electrical conductivity was assessed from aqueous BC suspensions prepared from purified BC samples. A total of 1 g of BC was dispersed in 100 mL of distilled water and homogenised before measurement. The electrical conductivity was recorded using a calibrated conductivity meter at intervals of 0, 1, 3, and 5 minutes, employing a water quality meter (AZ-86031, AZ Instrument Corp., Taiwan). The conductivity of distilled water was measured separately to establish a background value. The corrected conductivity for each BC suspension was obtained by subtracting the conductivity of the distilled water control from the measured conductivity of the respective suspension. Measurements were conducted using three independent biological replicates.

2.8 Mass Loss during Soil Burial

The resistance of BC to mass loss during soil burial was assessed using a soil-burial assay. Dried BC specimens were weighed prior to burial to determine their initial dry mass. Following this, the specimens were buried in soil at a depth of approximately 7 cm and incubated for a duration of 10 days under controlled experimental conditions. The soil used was sandy loam, characterised by a moisture content of 50%, a temperature of 25±2°C, a pH of 6.8±2, and an organic matter content of approximately 3%. It was subjected to aerobic incubation conditions. Following the incubation period, the specimens were carefully retrieved and gently washed with distilled water to eliminate any adhering soil particles. Great care was taken during both the retrieval and washing processes to minimise the potential loss of fragmented material. The recovered specimens were then dried to a constant mass before being weighed to determine their final dry mass. The percentage mass loss (ML) was subsequently calculated using Eq. (3).

$$\mathrm{ML}(\%) = \frac{m_i - m_f}{m_i} \times 100\% \qquad (3)$$

The initial dry mass is denoted as m_i, while the final dry mass after soil burial is represented as m_f. The results were presented as mass loss during soil burial instead of being classified directly as biodegradability. This approach is taken because the reduction in mass observed during a soil-burial experiment may arise not only from biological degradation but also from factors such as fragmentation,

retrieval losses, washing losses, and sample handling. Each treatment was assessed using three independent biological replicates.

2.9 Scanning Electron Microscopy (SEM)

The surface morphology of BC films was examined using SEM (JSM-6360LA, JEOL, Japan). For each cultivation strategy, the treatment showing the highest BC yield was selected for morphological analysis. The selected samples were dried to constant weight, mounted on specimen stubs, and sputter-coated with a conductive layer prior to observation. SEM images were acquired at appropriate magnifications to characterise the surface morphology and fibrillar structure of the BC network. Because the selected samples may differ in molasses concentration, the SEM observations were interpreted as treatment-specific morphological characteristics rather than as isolated effects of cultivation strategy.

2.10 Fourier Transform Infrared (FTIR) Analysis

FTIR analysis was performed to characterise the functional groups present in the selected BC samples using an FTIR spectrometer (Shimadzu 8201 PC, Japan) over the 4000–400 cm^{-1} wavenumber range. For each cultivation strategy, the treatment showing the highest BC yield was selected for analysis. The spectra were interpreted based on characteristic absorption bands associated with cellulose and other relevant functional groups. FTIR analysis was used to assess the chemical functional-group profiles of the selected samples; cellulose crystallinity or polymorphism was not assigned solely from the FTIR spectra. Because the selected samples may differ in molasses concentration, the observed spectral differences were interpreted as treatment-associated characteristics rather than as effects of cultivation strategy alone.

2.11 Statistical Analysis

All experiments were performed in triplicate, and the results are expressed as mean ± standard deviation (SD). Two-way and Three-Way analysis of variance (ANOVA) and Tukey's Test was performed using GraphPad Prism 9 and SPSS to determine the effects of molasses concentration and cultivation time on the measured properties of bacterial cellulose (BC). The interaction between the two factors was also evaluated. Statistical significance was determined at $p < 0.05$.

3. Results and Discussions

3.1 Effects of Molasses Concentration and Cultivation Strategy on BC Yield

Substrate composition and cultivation conditions influence BC biosynthesis. Table 1 presents BC yields across the 16 treatment combinations, evaluated using the factorial statistical model described in the Methods.

Table 1. Interactive effects of molasses concentration and cultivation strategy (static and agitation) on BC yield (g L^{-1})

Molasses concentration (%)	Static condition	Cultivation strategy using agitation		
		100 rpm	150 rpm	200 rpm
3	7.10 ± 0.10^{b}	47.30 ± 0.26^{a}	2.30 ± 0.10^{d}	3.20 ± 0.10^{c}
6	24.00 ± 0.20^{c}	51.50 ± 0.26^{a}	3.80 ± 0.10^{d}	22.10 ± 0.20^{b}
9	21.40 ± 0.20^{c}	48.70 ± 0.20^{a}	2.70 ± 0.10^{d}	28.20 ± 0.20^{b}
12	23.20 ± 0.20^{c}	49.10 ± 0.20^{a}	2.50 ± 0.10^{d}	42.40 ± 0.20^{b}

Note: Values are mean ± SD ($n = 3$, independent biological replicates). Different lowercase letters within the same row indicate statistically significant differences between cultivation strategies at the same molasses concentration according to Tukey's multiple comparisons test ($p < 0.05$).

Bacterial cellulose (BC) yield was calculated based on the dry weight of purified BC according to Equation (1). The yield was determined separately for each biological replicate, and the resulting values were averaged to obtain the final BC yield. For example, as illustrated in Table 1, a dry BC mass of 5.12 g obtained from 100 mL of molasses-based culture medium corresponds to a BC yield of 51.20 g L^{-1}, calculated by dividing the dry BC mass by the culture volume (0.1 L). As shown in Table 1, bacterial cellulose (BC) yield varied across molasses concentrations and cultivation strategies. Two-way ANOVA showed significant effects of cultivation strategy (F (3.32) = 137.434, $p < 0.0001$), molasses concentration (F (3.32) = 13.989, $p < 0.0001$), and their interaction (F (9.32) = 5.616, $p < 0.0001$). Cultivation strategy accounted for most of the total variation (81.67%), followed by the interaction (10.01%) and molasses concentration (8.31%). Tukey's multiple comparisons test indicated that all pairwise differences among cultivation strategies were significant within each molasses concentration ($p <$ 0,0001). Agitation at 100 rpm gave the highest yield at every concentration (47,30–51.50 g L^{-1}), with a maximum of 51.50 ± 0.26 g L^{-1} at 6% (w/v) molasses, whereas 150 rpm gave the lowest yields (2.30–3.80 g L^{-1}). The ranking of the static and 200 rpm conditions depended on molasses concentration; yield under static conditions was higher at 3% and 6% molasses, but lower at 9% and 12%. Numerically, static yield increased from 7.10 g L^{-1} at 3% to 24.00 g L^{-1} at 6%, whereas at 200 rpm yield increased with molasses concentration, reaching 42.40 g L^{-1} at 12%. Together with the significant interaction, these contrasting patterns indicate that the correlation between molasses concentration and BC yield depended on the cultivation strategy. Although agitation may influence mixing, oxygen availability, and hydrodynamic stress, these factors were not measured in this study and therefore cannot be established as the causes of the observed differences (Andrade *et al.,* 2020; Lahiri *et al.,* 2021).

The reported yields should also be interpreted in relation to the substrate basis and dry-mass calculation. Based on the reported total sugar content of molasses (17.39%), a 6% (w/v) molasses concentration provides approximately 10.43 g L^{-1} total sugar, making the reported yield of 51.50 g L^{-1} important to verify against the substrate input and yield calculation. Molasses composition may also influence fermentation performance because it contains sugars and other constituents (Ji *et al.,* 2016; Tyagi & Suresh, 2016). Therefore, 6% molasses at 100 rpm represents the treatment with the highest reported BC yield in this dataset, but confirmation of the calculation basis and mass balance is needed before interpreting this value as production efficiency.

3.2 Mechanical Properties of BC

Beyond BC yield, tensile strength and Young's modulus were evaluated to assess the effects of molasses concentration and cultivation strategy on BC mechanical performance (Tables 2 and 3).

Table 2. Effects of molasses concentration and cultivation strategy on the tensile strength (Mpa).

Molasses concentration (%)	Static condition	Cultivation strategy using agitation		
		100 rpm	150 rpm	200 rpm
3	22.45	46.10	4.20	2.34
6	45.80	51.60	28.10	38.40
9	42.10	45.50	2.10	43.20
12	35.60	45.20	6.40	52.80

Table 3. Effects of molasses concentration and cultivation strategy on Young's modulus (Mpa).

Molasses concentration (%)	Static condition	Cultivation strategy using agitation		
		100 rpm	150 rpm	200 rpm
3	280.50	640.79	55.30	28.50
6	645.89	695.13	340.60	490.20
9	580.19	635.40	30.20	595.60
12	420.15	630.10	85.90	720.40

Tensile strength and Young's modulus varied across molasses concentrations and cultivation strategies (Tables 2 and 3). Tensile strength ranged from 2.10 to 52.80 MPa, while Young's modulus ranged from 28.50 to 720.40 MPa. The highest values for both properties were recorded at 12% (w/v) molasses and 200 rpm, reaching 52.80 MPa and 720.40 MPa, respectively. At 100 rpm, both properties remained relatively high across the tested molasses concentrations, with a tensile strength of 45.20–51.60 MPa and a Young's modulus of 630.10–695.13 MPa. In contrast, the lowest values for both properties occurred at 150 rpm for the 3% and 9% molasses treatments.

The treatment with the highest reported BC yield (6% molasses at 100 rpm) also exhibited high tensile strength (51.60 MPa) and Young's modulus (695.13 MPa), although the maximum mechanical values occurred at 12% molasses and 200 rpm. This difference indicates that the treatment associated with the highest reported yield did not coincide with that producing the highest mechanical values. Similar variation in BC performance across cultivation conditions has been discussed in previous studies (Cakar *et al.*, 2014; Fabijanski & Garbarski, 2026). Although differences in fibril organisation and crystallinity may be relevant to mechanical behaviour, these structural characteristics were not directly quantified in this study; thus, the observed differences are interpreted as treatment-related variations rather than evidence of a specific structural mechanism.

3.3 Conductivity of BC

The electrical conductivity of hydrated BC suspensions was measured to assess the effects of molasses concentration and cultivation strategy. The conductivity response may reflect ionic transport through the hydrated BC network and is presented in Figure 1.

The electrical conductivity of hydrated BC suspensions varied with molasses concentration, cultivation strategy, and measurement time (Figure 1). Conductivity generally increased during the initial measurement period before approaching a relatively stable response. Higher values were generally observed at 9–12% molasses, while BC produced at 200 rpm exhibited the highest conductivity. Multiple linear regression showed significant associations between conductivity and molasses concentration, agitation speed, and measurement time (Table 4; $p < 0.05$). Among these variables, agitation speed had the largest standardised coefficient ($\beta = 0.616$), followed by molasses concentration ($\beta = 0.444$) and measurement time ($\beta = 0.197$).

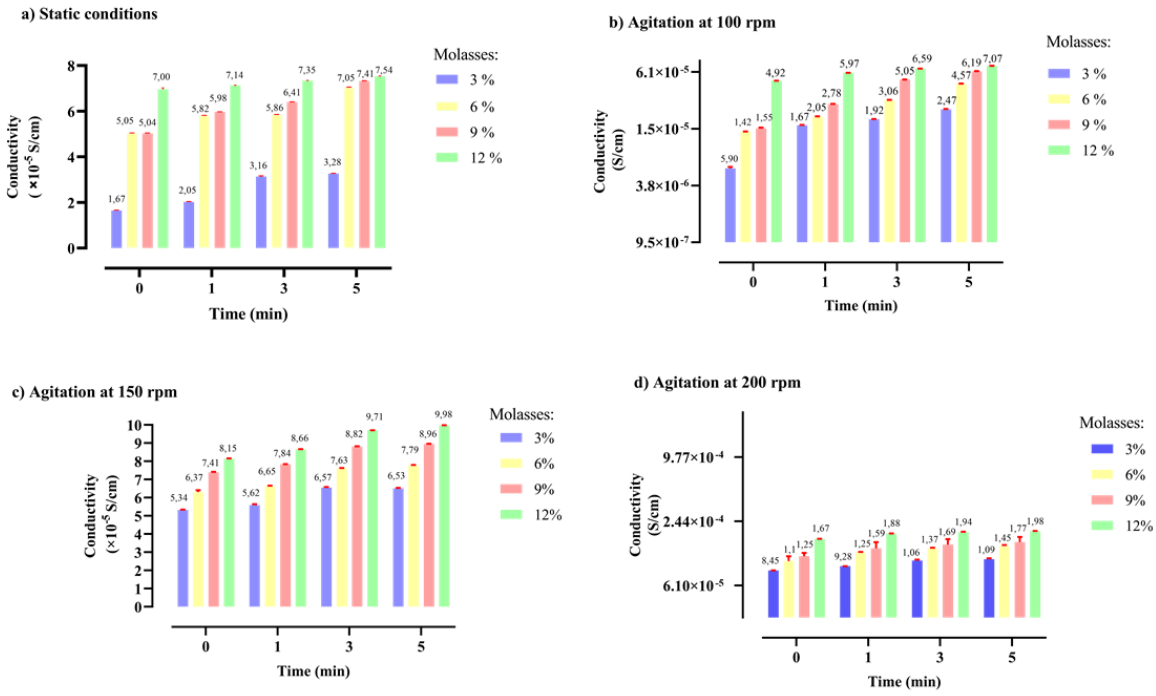

Figure 1. Time-dependent conductivity of BC produced under different molasses concentrations and cultivation strategies: (a) static cultivation, (b) agitation at 100 rpm, (c) agitation at 150 rpm, and (d) agitation at 200 rpm.

Table 4. Effects of cultivation strategy, molasses concentration, and contact time on the conductivity of BC.

Variable	Regression Coefficient	Standardized Coefficient	*t*-value	Significance
Molase (%)	4.993×10^{-6}	0.444	5.557	<0.001
Agitation (rpm)	3.141 × 10-7	0.616	7.708	<0.001
Time (min)	3.874 × 10-6	0.197	2.469	<0.016

These results indicate that conductivity was associated with both cultivation conditions and measurement time. However, because ionic composition, moisture distribution, and pore structure were not independently characterised, the differences cannot be attributed to a specific transport mechanism or structural change. Accordingly, conductivity is best interpreted as a treatment-dependent response of the hydrated BC suspensions rather than an intrinsic property of cellulose alone (Fang *et al.,* 2025; Fuentes *et al.,* 2001; Moghadas *et al.,* 2025).

3.4 Water Arbsorption Capacity (WAC) and Water Holding Capacity (WHC) of BC

WAC and WHC were evaluated to assess the hydration properties of BC, with results presented in Table 5.

Table 5. WAC and WHC of BC produced under different cultivation strategies.

Molasses	Strategy	WAC (%)				WHC (%)
(%)	(Agitation)	0.5 min	1 min	3 min	5 min	
3	0 rpm	15.62 ± 1.76^{dC}	32.93 ± 1.55^{cC}	49.16 ± 1.28^{bC}	56.57 ± 1.37^{aC}	51.67 ± 0.014^{b}
6	0 rpm	6.12 ± 0.44^{dC}	10.40 ± 0.46^{cBC}	13.81 ± 0.55^{bB}	15.65 ± 0.54^{aB}	55.33 ± 0.019^{b}
9	0 rpm	3.78 ± 0.46^{dB}	9.73 ± 0.57^{cB}	13.78 ± 0.52^{bB}	17.70 ± 0.47^{aB}	47.83 ± 0.155^{d}
12	0 rpm	4.99 ± 0.51^{dB}	20.20 ± 0.36^{cB}	23.15 ± 0.30^{bB}	26.03 ± 0.39^{aB}	40.08 ± 0.060^{c}

3	100 rpm	3.28 ± 0.22^{dC}	8.13 ± 0.21^{cD}	11.75 ± 0.21^{bD}	15.63 ± 0.20^{aD}	60.25 ± 0.016^{a}
6	100 rpm	5.05 ± 0.23^{dC}	7.39 ± 0.20^{cC}	10.71 ± 0.20^{bC}	14.27 ± 0.19^{aB}	47.92 ± 0.052^{c}
9	100 rpm	4.66 ± 0.27^{dB}	10.97 ± 0.22^{cB}	13.56 ± 0.23^{bB}	15.76 ± 0.22^{aB}	48.50 ± 0.067^{c}
12	100 rpm	4.37 ± 0.22^{dBC}	7.51 ± 0.22^{cC}	12.48 ± 0.21^{bC}	15.80 ± 0.20^{aC}	23.83 ± 0.030^{d}
3	150 rpm	66.86 ± 8.95^{cA}	107.23 ± 1.66^{bA}	176.17 ± 1.52^{aA}	176.38 ± 1.67^{aB}	45.00 ± 0.033^{c}
6	150 rpm	35.77 ± 2.64^{aA}	43.54 ± 2.58^{aA}	53.83 ± 1.95^{aA}	46.57 ± 13.59^{aA}	40.67 ± 0.030^{d}
9	150 rpm	98.08 ± 1.93^{cA}	151.46 ± 0.90^{bA}	198.39 ± 2.41^{aA}	201.69 ± 2.53^{aA}	55.25 ± 0.016^{b}
12	150 rpm	100.46 ± 0.91^{dA}	111.12 ± 0.04^{cA}	134.17 ± 0.84^{bA}	138.74 ± 0.79^{aA}	46.92 ± 0.032^{b}
3	200 rpm	48.22 ± 3.09^{cB}	76.05 ± 1.98^{bB}	98.83 ± 17.07^{bB}	198.33 ± 2.23^{aA}	40.75 ± 0.120^{d}
6	200 rpm	9.83 ± 0.51^{dB}	11.13 ± 0.50^{cB}	12.72 ± 0.50^{bBC}	24.02 ± 0.38^{aB}	56.08 ± 0.217^{a}
9	200 rpm	6.24 ± 0.40^{cB}	6.43 ± 0.42^{cC}	9.29 ± 0.36^{bC}	16.79 ± 0.32^{aB}	56.00 ± 0.247^{a}
12	200 rpm	2.94 ± 0.31^{cC}	5.72 ± 0.28^{bD}	6.44 ± 0.65^{bD}	12.14 ± 0.26^{aD}	56.83 ± 0.040^{a}

Note: Values are mean ± SD (n = 3, independent biological replicates). Lowercase letters indicate significant differences among time points within the same row, whereas uppercase letters indicate significant differences among cultivation strategies within the same column, at the same molasses concentration and soaking time. Different letters indicate statistically significant differences according to Tukey's significant test ($p < 0.05$).

Water absorption capacity (WAC) generally increased with immersion time across most treatment combinations. However, the magnitude of this increase varied with molasses concentration and cultivation strategy. At 150 rpm, WAC did not differ significantly between 3 and 5 min at 3% and 9% molasses. Similarly, at 200 rpm, no significant differences were observed between 1 and 3 min at 3% molasses, between 0.5 and 1 min at 9% molasses, or between 1 and 3 min at 12% molasses. At 6% molasses, WAC did not differ significantly across immersion times under the 150-rpm condition. Overall, the 150-rpm treatment exhibited the highest WAC in 15 of the 16 molasses concentration–time combinations. The only exception occurred at 3% molasses after 5 min, when the 200-rpm treatment exhibited a higher WAC (198.33%) than the 150-rpm treatment (176.38%). At 3% molasses, static cultivation and cultivation at 100 rpm generally exhibited the lowest WAC values. In contrast, WHC showed a different treatment pattern. Water-holding capacity (WHC) ranged from 23.83 ± 0.030 % at 12 % (w/v) molasses and 100 rpm to 60.25 ± 0.016 % at 3 % (w/v) molasses and 100 rpm. Two-way analysis of variance (ANOVA) revealed significant effects of molasses concentration (F (3.32) = 22.582, $p < 0.0001$), cultivation strategy (F (3.32) = 11.321, $p < 0.0001$), and the interaction between these factors (F (9.32) = 29.024, $p < 0.0001$). The interaction accounted for the largest proportion of the total variation (71.97%), followed by molasses concentration (18.67%) and cultivation strategy (9.36%). Given the significant interaction, the effect of cultivation strategy on WHC should be interpreted within each molasses concentration. Tukey's multiple-comparison test indicated that all cultivation strategies differed significantly from one another at each molasses concentration ($p < 0.0001$). The ranking of the cultivation strategies varied with molasses concentration: 100 rpm resulted in the highest WHC at 3% (w/v) molasses but the lowest at 12% (w/v), whereas 200 rpm produced the highest WHC at 6%, 9%, and 12% (w/v) molasses and the lowest at 3% (w/v). These crossing response patterns are consistent with the significant interaction between cultivation strategy and molasses concentration, indicating that the effect of cultivation strategy on WHC depended on molasses concentration and that no single strategy consistently produced the highest WHC across all conditions. These results show that the conditions associated with maximum water absorption did not coincide with those producing maximum water retention.

The contrasting WAC and WHC patterns indicate that water uptake during immersion and water retention after the WHC test represent distinct hydration properties of BC (Chen *et al.,* 2026; Portela *et al.,* 2019; Priscila *et al.,* 2025). The variation across treatments may be related to differences in the

material's physical structure; however, pore architecture and fibril organisation were not quantitatively characterised, so their specific contributions cannot be established. Under the tested conditions, 9% molasses at 150 rpm gave the highest WAC, whereas 3% molasses at 100 rpm gave the highest WHC.

3.5 Mass Loss During Soil Burial

Mass loss during soil burial was evaluated to assess the biodegradability of BC under environmental conditions. The results are presented in Table 6.

Table 6. Effects of molasses concentration and cultivation strategy on the mass loss during soil burial of BC (%).

Molasses concentration (%)	Static condition	Cultivation strategy using agitation		
		100 rpm	150 rpm	200 rpm
3	79.85±0.172^{d}	92.46±0.122^{c}	97.37±0.002^{b}	97.80±0.001^{a}
6	57.55±0.198^{d}	91.00±0.077^{a}	87.42±0.089^{b}	83.84±0.247^{c}
9	65.11±0.206^{c}	99.85±0.001^{a}	97.90±0.000^{b}	97.98±0.001^{b}
12	89.24±0.059^{d}	99.80±0.000^{a}	95.29±0.048^{c}	98.01±0.001^{b}

Note: Values are mean ± SD (n = 3, independent biological replicates). Different lowercase letters within the same row indicate significant differences among cultivation strategies at the same molasses concentration according to Tukey's multiple comparisons test ($p < 0.05$)

Mass loss during the 10-day soil-burial test varied across molasses concentrations and cultivation strategies (Table 6). The observed mass loss ranged from 57.55 ± 0.198 to 99.85 ± 0.001%. Two-way analysis of variance (ANOVA) revealed significant main effects of cultivation strategy (F (3.32) = 112.276, $p < 0.0001$) and molasses concentration (F (3.32) = 41.561, $p < 0.0001$), as well as a significant interaction between these factors (F (9.32) = 9.302, $p < 0.0001$). Cultivation strategy accounted for the largest proportion of the total variation (61.77 %), followed by molasses concentration (22.87 %) and the interaction between cultivation strategy and molasses concentration (15.35 %). Tukey's post hoc multiple-comparison test revealed significant differences among cultivation strategies at each molasses concentration, except between the 150 and 200 rpm treatments at 9 % (w/v) molasses ($p = 0.824$). Static cultivation exhibited the lowest mass loss across all molasses concentrations, with the minimum observed at 6 % (w/v) molasses. In contrast, the maximum mass loss was recorded at 9% (w/v) molasses under agitation at 100 rpm. Mass loss in all agitated treatments ranged from 83.84 % to 99.85 %. The agitation speed associated with the highest mass loss varied according to molasses concentration, with 200 rpm producing the highest value at 3 % molasses and 100 rpm producing the highest values at 6, 9, and 12 % molasses. The significant interaction indicates that the effect of cultivation strategy on mass loss varied depending on molasses concentration. Furthermore, mass loss did not follow a consistent trend with increasing molasses concentration or agitation speed.

The observed differences may reflect treatment-associated variations in the BC specimens; however, the specific factors responsible were not determined in this study. Mass loss during soil burial can also include material lost through fragmentation, retrieval, and washing, and therefore should not be interpreted solely as biodegradation (Aydin *et al.*, 2026; Melro *et al.*, 2025). Accordingly, the observed changes are reported as mass loss under the soil-burial conditions used in this study, as mass loss alone does not provide direct evidence of biodegradation.

3.6 Surface Morphology of BC

SEM was used to examine the surface morphology of BC and assess microstructural differences associated with cultivation strategy (Figure 2). Because fibril assembly is influenced by fermentation conditions, these morphological features may contribute to differences in the physicochemical and functional properties of BC.

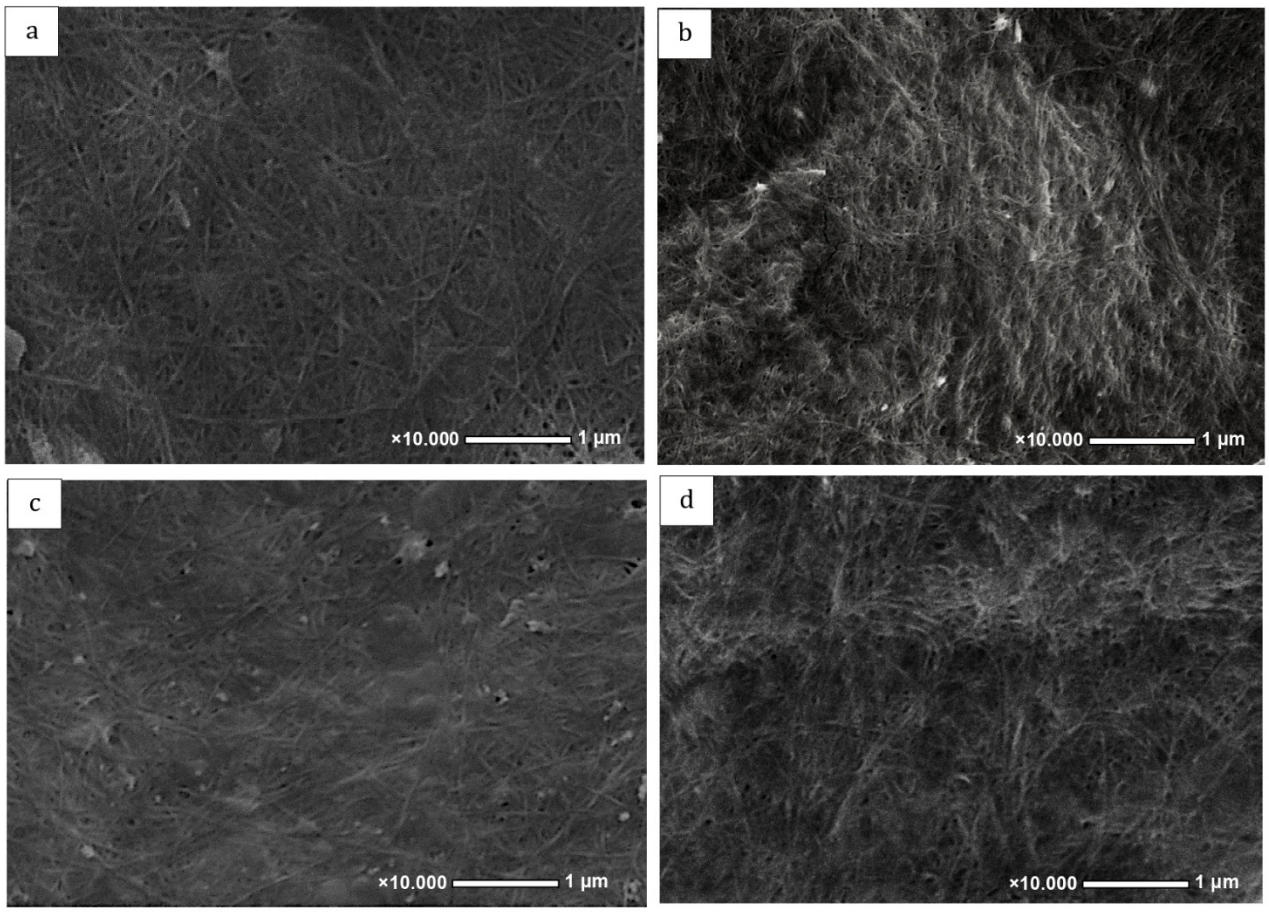

Figure 2. SEM images of BC produced under the highest-yielding treatment within each cultivation mode: (a) static cultivation with 6% (w/v) molasses, (b) 100 rpm with 6% molasses, (c) 150 rpm with 6% molasses, and (d) 200 rpm with 12% molasses (10,000× magnification)

SEM was used to characterise the apparent surface morphology of BC from the selected highest-yielding treatment within each cultivation mode (Figure 2). The selected samples exhibited distinct morphological features. The static sample showed relatively compact, smooth fibers, randomly oriented in different directions, forming a relatively homogeneous fibrous network with small pores distributed between the fibers. In contrast, the 100-rpm sample exhibited a more heterogeneous surface morphology, characterized by overlapping and aggregated fibers in certain regions, while other areas displayed a looser fiber arrangement with numerous small pores distributed throughout the network. The 150-rpm sample exhibited a less ordered surface with irregular fibril arrangement and localised aggregates, while the 200-rpm sample showed a comparatively dense fibrillar structure (Sarkono *et al.,* 2014). These morphological characteristics were broadly associated with the measured material properties. The interconnected structure observed at 100 rpm coincided with the highest BC yield, whereas the denser structure at 200 rpm corresponded to the highest tensile strength and Young's modulus. However, these relationships should be interpreted as associations rather than causal effects because fibril density, pore size, and pore connectivity were not quantitatively determined. In addition, the selected samples differed in molasses concentration, with the 200-rpm sample produced using 12% molasses. Therefore, the observed morphological differences cannot be attributed solely to cultivation strategy. Comparative SEM analysis using a common molasses concentration would be required to isolate the specific effect of agitation on BC morphology.

3.7 FTIR Analysis

FTIR spectroscopy was used to characterise the functional groups and chemical bonding environments of BC produced under different cultivation strategies (Figure 3). This analysis assessed whether cultivation conditions caused major changes in cellulose-associated functionalities.

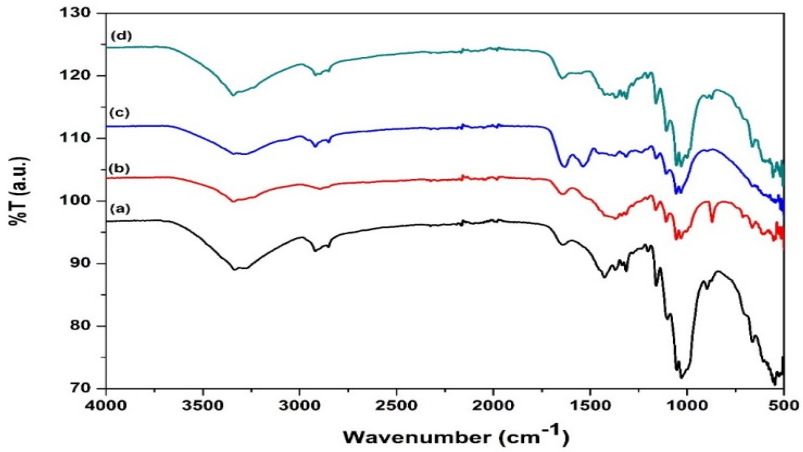

Figure 3. FTIR spectra of BC obtained from the highest-yielding treatment within each cultivation mode: (a) static cultivation with 6% (w/v) molasses, (b) 100 rpm with 6% molasses, (c) 150 rpm with 6% molasses, and (d) 200 rpm with 12% molasses.

FTIR spectroscopy was used to characterise the functional groups of BC produced under the selected cultivation conditions (Figure 3). All spectra exhibited characteristic cellulose-associated absorption bands, confirming the retention of the cellulose-related chemical structure across the treatments. The broad O–H stretching band occurred at 3336.28, 3342.84, 3286.75, and 3342.77 cm^{-1} for the static, 100-, 150-, and 200-rpm samples, respectively, reflecting the hydroxyl-rich structure of cellulose and its hydrogen-bonding environment (Espindola *et al.,* 2021; Lull *et al.,* 2022). Absorption bands in the 1029–1161 cm^{-1} region were associated with C–O and C–O–C stretching vibrations of the cellulose backbone (Cristina *et al.,* 2026; Luiz *et al.,* 2023). Although differences in band position and relative intensity were observed, the overall spectral profiles were qualitatively similar, indicating no major qualitative changes in the cellulose-associated functional groups. A distinct band at 1631.35 cm^{-1} was observed only in the 150-rpm sample. This region may be associated with absorbed water and can overlap with signals from carbonyl-containing or other non-cellulosic components; therefore, its specific origin cannot be determined from FTIR alone. The C–H-related features were more evident in the static and 100-rpm samples but less pronounced at 150 and 200 rpm; however, these qualitative intensity differences may also be affected by sample preparation and measurement conditions.

Overall, the spectra retained the characteristic cellulose-associated functional groups, with no clear evidence of major qualitative changes among the selected samples. However, FTIR alone cannot establish differences in crystallinity, polymorphism, or degree of polymerisation. Interpretation of spectral differences is also limited because the samples were selected from the highest-yielding treatment within each cultivation strategy, and the 200-rpm sample contained 12% molasses while the other samples contained 6%. Therefore, the observed differences should be interpreted as treatment-associated characteristics rather than effects of agitation alone.

4. Conclusions

Overall, this study demonstrated that sugarcane molasses concentration and cultivation strategy significantly influenced bacterial cellulose (BC) yield and functional properties ($p < 0.05$). The highest reported BC yield was obtained at 6% (w/v) molasses and 100 rpm, whereas the highest tensile strength

and Young's modulus were recorded at 12% molasses and 200 rpm. The highest water absorption capacity was observed at 9% molasses and 150 rpm, while the highest water-holding capacity occurred at 3% molasses under 100 rpm agitation. Conductivity and mass loss during soil burial also varied among treatments. FTIR spectra retained characteristic cellulose-associated functional groups, although treatment-related spectral differences could not be attributed to agitation alone. Overall, the results indicate that the treatment associated with the highest reported yield did not produce the maximum values for all functional properties. However, the reported BC yield requires verification against the substrate mass balance, and the factorial statistical analysis should be confirmed before drawing definitive conclusions about the individual effects of molasses concentration, cultivation strategy, and their interaction.

5. Acknowledgment and Funding Information

The authors appreciate the Biology Advance Laboratory, Physic Advance Laboratory, and Environment Laboratory, University of Mataram, as well as the Integrated Laboratory, UIN Mataram, for providing facilities and assistance in analysis. This research did not receive any specific grant from funding agencies in the public, commercial, or not-for-profit sectors

6. Conflict of Interest Declaration

The authors declare that there is no conflict of interest regarding to the publication of this article. The authors confirm that the paper was free of plagiarism.

7. Author Contribution Statement

This journal uses Contributor Roles Taxonomy (CRediT) to recognize individual author contributions, reduce authorship disputes, and facilitate collaboration.

Name of Author	C	M	So	Va	Fo	I	R	D	O	E	Vi	Su	P	Fu
Nurrijawati Nurrijawati			x		x	x				x	x			
Sarkono Sarkono		x		x				x		x				
Dhony Hermanto		x							x	x	x			

C: **C**onceptualization
M : **M**ethodology
So : **So**ftware
Va : **Va**lidation
Fo : **Fo**rmal analysis
I : **I**nvestigation
R : **R**esources
D : **D**ata Curation
O : Writing - **O**riginal Draft
E : Writing - Review & **E**diting
Vi : **Vi**sualization
Su : **Su**pervision
P : **P**roject administration
Fu : **Fu**nding acquisition

8. Generative AI Statement

During the preparation of this manuscript, the authors used Grammarly and ChatGPT (OpenAI) to assist with English grammar correction, language refinement, paraphrasing, and improving the manuscript's clarity and readability. The authors critically reviewed, edited, and validated all AI-generated suggestions to ensure accuracy, originality, and scientific integrity. Generative AI was used solely as a supportive tool and was not involved in generating original experimental data or independently conducting statistical analyses or interpreting research findings. The authors take full responsibility for the accuracy, integrity, and final content of the manuscript. Generative AI tools are not credited with authorship.

9. References

Alidu, M., & Alexander, S. L. M. (2026). Bacterial Cellulose Production : Decoupling Yield and Structural Quality in Refined and Waste-Derived Carbon Sources. *Fermentation*, *12*(336), 1–33. https://doi.org/10.3390/fermentation12070336

Amorim, J., Liao, K., Mandal, A., Costa, D. S., Roumeli, E., & Sarubbo, L. A. (2024). Impact of Carbon Source on Bacterial Cellulose Network Architecture and Prolonged Lidocaine Release. *Polymer*, *16*, 3021. https://doi.org/10.3390/polym16213021

Andrade, I. De, Fernandes, A., Cristina, A., Rampazzo, V., Gonçalves, D., Sarah, M., Ozaki, C., Maria, G., Windson, C., & Haminiuk, I. (2020). Bacterial cellulose : From production optimization to new applications. *International Journal of Biological Macromolecules*, *164*, 2598–2611. https://doi.org/10.1016/j.ijbiomac.2020.07.255

Aydin, M. S., Yamada, S., Mohamed-ahmed, S., Rashad, A., & Mustafa, K. (2026). Influence of scaffold porosity on the degradation of 3D-printed biodegradable polymers : Coupled bioreactor , modeling , and in vivo validation. *Materials Today Advances*, *30*, 100804. https://doi.org/10.1016/j.mtadv.2026.100804

Cakar, F., Ozer, I., Aytekin, A. Ö., & Fikrettin, S. (2014). Improvement production of bacterial cellulose by semi-continuous process in molasses medium. *Carbohydrate Polymers*, *106*, 7–13. https://doi.org/10.1016/j.carbpol.2014.01.103

Çalhan, A., & Hasanoğlu, A. (2026). Bacterial cellulose as a next - generation membrane material for selective transport: properties, fabrication, and applications. In *Cellulose* (Vol. 33, Issue 3). Springer Netherlands. https://doi.org/10.1007/s10570-025-06926-9

Chen, H., Huang, Y., Wang, F., Fu, Z., Li, A., Abdelsadig, M., Brassil, M., Xia, Y., Zhou, B., Du, G., & Fan, M. (2026). Recent advances in nanocellulose scaffold membranes : Sources , processing and functionalization. *Materials Today Bio*, *38*, 103221. https://doi.org/10.1016/j.mtbio.2026.103221

Cristina, A., Martins, D., Silva-carvalho, R., Marques, S., Dourado, F., & Gama, M. (2026). Nanobubble-enhanced oxygen transfer in bacterial nanocellulose production : Comparative evaluation with static and airlift systems. *International Journal of Biological Macromolecules*, *346*, 150572. https://doi.org/10.1016/j.ijbiomac.2026.150572

Espindola, S. P., Pronk, M., Zlopasa, J., Picken, S. J., & Loosdrecht, M. C. M. Van. (2021). Nanocellulose recovery from domestic wastewater. *Journal of Cleaner Production*, *280*, 124507. https://doi.org/10.1016/j.jclepro.2020.124507

Fabijanski, M., & Garbarski, J. (2026). The Influence of Cellulose Fiber Content on the Mechanical Properties of Composites Based on Modified Thermoplastic Starch. *Processes*, *14*(1480), 1–16. https://doi.org/10.3390/pr14091480

Fang, L., Zhou, Y., & Huang, Q. (2025). Ionic Conductive Textiles for Wearable Technology. *Advances Materials*, *37*, 2502140. https://doi.org/10.1002/adma.202502140

Fuentes, R. O., Figueiredo, F. M., Marques, F. M. B., & Franco, J. I. (2001). Influence of microstructure on the electrical properties of NASICON materials. *Solis State Ionics*, *140*, 173–179. https://doi.org/10.1016/S0167-2738(01)00701-9

Gomes, P., Silva, N. H. C. S., Trovatti, E., Duarte, M. F., Silvestre, A. J. D., Pascoal, C., & Freire, C. S. R. (2013). Production of bacterial cellulose by Gluconacetobacter sacchari using dry olive mill residue. *Biomass and Bioenergy*, *55*, 205–211. https://doi.org/10.1016/j.biombioe.2013.02.004

Hapsari, D. P., Perdani, C. G., Fahmi, F., Nurika, I., & Gunawan, S. (2024). BNC production of siwalan neer and sugarcane molasses as novel media sources. *Advances in Food Science, Sustainable Agriculture and Agroindustrial Engineering*, *7*(2), 141–149. https://doi.org/10.21776/ub.afssaae.2024.007.02.3

Ji, K., Wang, W., Zeng, B., Chen, S., Zhao, Q., Chen, Y., Li, G., & Ma, T. (2016). Bacterial cellulose synthesis mechanism of facultative anaerobe. *Scientific Reports*, *6*, 21863. https://doi.org/10.1038/srep21863

Kumar, U. V., Narayanasamy, S., & Uthandi, S. (2025). Bacterial cellulose: A comprehensive review on biosynthesis, sustainable production, and multifaceted industrial applications. *Food and Bioproducts Processing*, *154*, 153–174. https://doi.org/10.1016/j.fbp.2025.08.013

Lahiri, D., Nag, M., Dutta, B., Dey, A., Sarkar, T., & Pati, S. (2021). Bacterial Cellulose: Production, Characterization, and Application as Antimicrobial Agent. *International Journal of Molecular Sciences Review*, *22*(12984), 1–18. https://doi.org/10.3390/ijms222312984

López-lópez, E., Espinoza-casta, J. I., Martinez-mayorga, K., & Medina-franco, J. L. (2026). Structure – Property Associations : Breaking Paradigms for Linking Chemical Structures and Biological Properties in Drug Discovery. *ChemMedChem*, *21*, e202500847. https://doi.org/10.1002/cmdc.202500847

Luiz, W. H. A., Frajacomo, S. C. L., Yamada, C., & Lustri, W. R. (2023). Influence of carbon sources on the physicochemical properties and yield of bacterial cellulose production for drug delivery. *International Journal of Advances in Medical Biotechnology*, *5*(2), 40–50. https://doi.org/10.52466/ijamb.v5i2.117

Lull, F., Zahel, M., & Panzner, M. (2022). Fundamental investigations on the laser - melting of lignocellulosic fibres. *Cellulose*, *29*(14), 7587–7601. https://doi.org/10.1007/s10570-022-04702-7

Melro, L., Alves, C., Fernandes, M., Rocha, S., Mehravani, B., Ribeiro, A. I., Azevedo, S., & Cardoso, V. F. (2025). Bacterial nanocellulose as a versatile scaffold for biomedical applications : Synthesis , functionalization , and future prospects. *Applied Materials Today*, *46*, 102858. https://doi.org/10.1016/j.apmt.2025.102858

Mirshafiei, M., Afshar, A. K., Yazdian, F., Rashedi, H., Rahdar, A., & Aboudzadeh, M. A. (2026). Sustainability Bacterial cellulose : a sustainable nanostructured polymer for biosensor development. *RSC Sustainability*, *4*(178), 178–206. https://doi.org/10.1039/D5SU00426H

Moghadas, N., Ghadami, A., Rezavand, N., Shojaei, S., Tehrani, P., Hassan, S., Jafari-nodoushan, M., & Goodarzi, V. (2025). Development and characterization of a biocompatible aerogel composed of kombucha bacterial cellulose , Cu – Zn nanoparticles , and polypyrrole nanocomposites. *Inorganic Chemistry Communications*, *182*, 115476. https://doi.org/10.1016/j.inoche.2025.115476

Oesef, K., Cranston, E. D., & Abdin, Y. (2024). Current advances in processing and modification of cellulose nanofibrils for high-performance composite applications. *Materials & Design*, *247*, 113417. https://doi.org/10.1016/j.matdes.2024.113417

Parchaykina, M. V, Liyaskina, E. V, Bogatyreva, A. O., Baykov, M. A., Gotina, D. S., Arzhanov, N. E., Netrusov, A. I., & Revin, V. V. (2025). Cost-Effective Production of Bacterial Cellulose and Tubular Materials by Cultivating Komagataeibacter sucrofermentans B-11267 on a Molasses Medium. *Polymer*, *17*(179), 1–20. https://doi.org/10.3390/polym17020179

Portela, R., Leal, C. R., & Pedro, L. (2019). Minireview Bacterial cellulose : a versatile biopolymer for wound dressing applications. *Microbial Biotechnology*, *12*, 586–610. https://doi.org/10.1111/1751-7915.13392

Alidu, M., & Alexander, S. L. M. (2026). Bacterial Cellulose Production : Decoupling Yield and Structural Quality in Refined and Waste-Derived Carbon Sources. *Fermentation*, *12*(336), 1–33. https://doi.org/10.3390/fermentation12070336

Amorim, J., Liao, K., Mandal, A., Costa, D. S., Roumeli, E., & Sarubbo, L. A. (2024). Impact of Carbon Source on Bacterial Cellulose Network Architecture and Prolonged Lidocaine Release. *Polymer*, *16*, 3021. https://doi.org/10.3390/polym16213021

Andrade, I. De, Fernandes, A., Cristina, A., Rampazzo, V., Gonçalves, D., Sarah, M., Ozaki, C., Maria, G., Windson, C., & Haminiuk, I. (2020). Bacterial cellulose : From production optimization to new applications. *International Journal of Biological Macromolecules*, *164*, 2598–2611. https://doi.org/10.1016/j.ijbiomac.2020.07.255

Aydin, M. S., Yamada, S., Mohamed-ahmed, S., Rashad, A., & Mustafa, K. (2026). Influence of scaffold porosity on the degradation of 3D-printed biodegradable polymers : Coupled bioreactor , modeling

, and in vivo validation. *Materials Today Advances*, *30*, 100804. https://doi.org/10.1016/j.mtadv.2026.100804

Cakar, F., Ozer, I., Aytekin, A. Ö., & Fikrettin, S. (2014). Improvement production of bacterial cellulose by semi-continuous process in molasses medium. *Carbohydrate Polymers*, *106*, 7–13. https://doi.org/10.1016/j.carbpol.2014.01.103

Çalhan, A., & Hasanoğlu, A. (2026). Bacterial cellulose as a next - generation membrane material for selective transport: properties, fabrication, and applications. In *Cellulose* (Vol. 33, Issue 3). Springer Netherlands. https://doi.org/10.1007/s10570-025-06926-9

Chen, H., Huang, Y., Wang, F., Fu, Z., Li, A., Abdelsadig, M., Brassil, M., Xia, Y., Zhou, B., Du, G., & Fan, M. (2026). Recent advances in nanocellulose scaffold membranes : Sources , processing and functionalization. *Materials Today Bio*, *38*, 103221. https://doi.org/10.1016/j.mtbio.2026.103221

Cristina, A., Martins, D., Silva-carvalho, R., Marques, S., Dourado, F., & Gama, M. (2026). Nanobubble-enhanced oxygen transfer in bacterial nanocellulose production : Comparative evaluation with static and airlift systems. *International Journal of Biological Macromolecules*, *346*, 150572. https://doi.org/10.1016/j.ijbiomac.2026.150572

Espindola, S. P., Pronk, M., Zlopasa, J., Picken, S. J., & Loosdrecht, M. C. M. Van. (2021). Nanocellulose recovery from domestic wastewater. *Journal of Cleaner Production*, *280*, 124507. https://doi.org/10.1016/j.jclepro.2020.124507

Fabijanski, M., & Garbarski, J. (2026). The Influence of Cellulose Fiber Content on the Mechanical Properties of Composites Based on Modified Thermoplastic Starch. *Processes*, *14*(1480), 1–16. https://doi.org/10.3390/pr14091480

Fang, L., Zhou, Y., & Huang, Q. (2025). Ionic Conductive Textiles for Wearable Technology. *Advances Materials*, *37*, 2502140. https://doi.org/10.1002/adma.202502140

Fuentes, R. O., Figueiredo, F. M., Marques, F. M. B., & Franco, J. I. (2001). Influence of microstructure on the electrical properties of NASICON materials. *Solis State Ionics*, *140*, 173–179. https://doi.org/10.1016/S0167-2738(01)00701-9

Gomes, P., Silva, N. H. C. S., Trovatti, E., Duarte, M. F., Silvestre, A. J. D., Pascoal, C., & Freire, C. S. R. (2013). Production of bacterial cellulose by Gluconacetobacter sacchari using dry olive mill residue. *Biomass and Bioenergy*, *55*, 205–211. https://doi.org/10.1016/j.biombioe.2013.02.004

Hapsari, D. P., Perdani, C. G., Fahmi, F., Nurika, I., & Gunawan, S. (2024). BNC production of siwalan neer and sugarcane molasses as novel media sources. *Advances in Food Science, Sustainable Agriculture and Agroindustrial Engineering*, *7*(2), 141–149. https://doi.org/10.21776/ub.afssaae.2024.007.02.3

Ji, K., Wang, W., Zeng, B., Chen, S., Zhao, Q., Chen, Y., Li, G., & Ma, T. (2016). Bacterial cellulose synthesis mechanism of facultative anaerobe. *Scientific Reports*, *6*, 21863. https://doi.org/10.1038/srep21863

Kumar, U. V., Narayanasamy, S., & Uthandi, S. (2025). Bacterial cellulose: A comprehensive review on biosynthesis, sustainable production, and multifaceted industrial applications. *Food and Bioproducts Processing*, *154*, 153–174. https://doi.org/10.1016/j.fbp.2025.08.013

Lahiri, D., Nag, M., Dutta, B., Dey, A., Sarkar, T., & Pati, S. (2021). Bacterial Cellulose: Production, Characterization, and Application as Antimicrobial Agent. *International Journal of Molecular Sciences Review*, *22*(12984), 1–18. https://doi.org/10.3390/ijms222312984

López-lópez, E., Espinoza-casta, J. I., Martinez-mayorga, K., & Medina-franco, J. L. (2026). Structure – Property Associations : Breaking Paradigms for Linking Chemical Structures and Biological Properties in Drug Discovery. *ChemMedChem*, *21*, e202500847. https://doi.org/10.1002/cmdc.202500847

Luiz, W. H. A., Frajacomo, S. C. L., Yamada, C., & Lustri, W. R. (2023). Influence of carbon sources on the physicochemical properties and yield of bacterial cellulose production for drug delivery.

International Journal of Advances in Medical Biotechnology, *5*(2), 40–50. https://doi.org/10.52466/ijamb.v5i2.117

Lull, F., Zahel, M., & Panzner, M. (2022). Fundamental investigations on the laser - melting of lignocellulosic fibres. *Cellulose*, *29*(14), 7587–7601. https://doi.org/10.1007/s10570-022-04702-7

Melro, L., Alves, C., Fernandes, M., Rocha, S., Mehravani, B., Ribeiro, A. I., Azevedo, S., & Cardoso, V. F. (2025). Bacterial nanocellulose as a versatile scaffold for biomedical applications : Synthesis , functionalization , and future prospects. *Applied Materials Today*, *46*, 102858. https://doi.org/10.1016/j.apmt.2025.102858

Mirshafiei, M., Afshar, A. K., Yazdian, F., Rashedi, H., Rahdar, A., & Aboudzadeh, M. A. (2026). Sustainability Bacterial cellulose : a sustainable nanostructured polymer for biosensor development. *RSC Sustainability*, *4*(178), 178–206. https://doi.org/10.1039/D5SU00426H

Moghadas, N., Ghadami, A., Rezavand, N., Shojaei, S., Tehrani, P., Hassan, S., Jafari-nodoushan, M., & Goodarzi, V. (2025). Development and characterization of a biocompatible aerogel composed of kombucha bacterial cellulose , Cu – Zn nanoparticles , and polypyrrole nanocomposites. *Inorganic Chemistry Communications*, *182*, 115476. https://doi.org/10.1016/j.inoche.2025.115476

Oesef, K., Cranston, E. D., & Abdin, Y. (2024). Current advances in processing and modification of cellulose nanofibrils for high-performance composite applications. *Materials & Design*, *247*, 113417. https://doi.org/10.1016/j.matdes.2024.113417

Parchaykina, M. V, Liyaskina, E. V, Bogatyreva, A. O., Baykov, M. A., Gotina, D. S., Arzhanov, N. E., Netrusov, A. I., & Revin, V. V. (2025). Cost-Effective Production of Bacterial Cellulose and Tubular Materials by Cultivating Komagataeibacter sucrofermentans B-11267 on a Molasses Medium. *Polymer*, *17*(179), 1–20. https://doi.org/10.3390/polym17020179

Portela, R., Leal, C. R., & Pedro, L. (2019). Minireview Bacterial cellulose : a versatile biopolymer for wound dressing applications. *Microbial Biotechnology*, *12*, 586–610. https://doi.org/10.1111/1751-7915.13392

Priscila, R., Catarino, F., Costa, L., & Spinosa, W. A. (2025). Sustainability and Influencing Factors in Bacterial Cellulose Production : A Review of the Impact of Microorganisms , Culture Media and Cultivation Methods. *Food Technology and Biotechnology*, *63*(3), 332–350. https://doi.org/10.17113/ftb.63.03.25.8746

Rezaei, N., Razavi, P., Mohammad, S., & Chackoshian, A. (2025). Food waste-derived bacterial cellulose biosorbents as a cost-effective solution for sustainable heavy metal and dye removal. *International Journal of Biological Macromolecules*, *330*, 147686. https://doi.org/10.1016/j.ijbiomac.2025.147686

Sarkono, Moeljopawiro, S., Setiaji, B., & Sembiring, L. (2014). Physico-chemical Properties of Bacterial Cellulose Produced by Newly Strain Gluconacetobacter xylinus ANG-29 in Static and Shaking Fermentations. *Biosciences Biotechnology Research Asia*, *11*(3), 1259–1265. https://doi.org/10.13005/bbra/1514

Turganova, R., Tuleyeva, R., Belkozhayev, A., & Gizatullina, N. (2025). Bacterial Cellulose for Sustainable Food Packaging: Production Pathways, Structural Design, and Functional Modification Strategies. *Polymer*, *17*(3165), 1–37. https://doi.org/10.3390/polym17233165

Tyagi, N., & Suresh, S. (2016). Production of cellulose from sugarcane molasses using Gluconacetobacter intermedius SNT-1 : optimization & characterization. *Journal of Cleaner Production*, *112*, 71–80. https://doi.org/10.1016/j.jclepro.2015.07.054

Wang, X., Yan, W., Srinuanpan, S., Quan, M., Ching, J., Xu, B., & Chuan, T. (2026). Co-culture engineering for sustainable bacterial cellulose manufacturing: Process intensification, functional materials and industrial translation. *Carbohydrate Polymer Technologies and Applications*, *15*, 101211. https://doi.org/10.1016/j.carpta.2026.101211

About Author(s)

Nurrijawati is a master's student in the Magister of Biology Program, Faculty of Mathematics and Natural Science, University of Mataram, Mataram, West Nusa Tenggara, Indonesia, where her research interests include bacterial cellulose, microbial physiology, fermentation technology, and biopolymers. ORCID ID: 0009-0000-0960-4001.

Dr. Sarkono is a lecturer in the Biology Department, Faculty of Mathematics and Natural Sciences, University of Mataram, Indonesia. He currently teaches courses including microbial physiology, food microbiology, and microbial ecology. He serves as the head of the Microbiology Research Group, with research interests in food microbiology—specifically concerning lactic acid bacteria and acetic acid bacteria. His current research focuses on cellulose-producing acetic acid bacteria for food applications. ORCID ID: 0009-0002-2915-4348.

Dr. Dhony Hermanto is a lecturer in the Chemistry Department, Faculty of Mathematics and Natural Science, University of Mataram, Mataram, West Nusa Tenggara, Indonesia, where his research interests include materials science, analytical chemistry, and sensors. ORCID ID: 0000-0001-6907-0021.